Molecular Cell, Vol. 16, 881–891, December 22, 2004, Copyright ©2004 by Cell Press

A Mechanism for the Potent Inhibition of Eukaryotic Acetyl-Coenzyme A Carboxylase by Soraphen A, a Macrocyclic Polyketide Natural Product

Yang Shen,[1] Sandra L. Volrath,[2] Stephanie C. Weatherly,[2] Tedd D. Elich,[2] and Liang Tong[1,*]
[1]Department of Biological Sciences
Columbia University
New York, New York 10027
[2]Cropsolution, Inc.
P.O. Box 14069
Research Triangle Park, North Carolina 27560

Summary

Acetyl-coenzyme A carboxylases (ACCs) have crucial roles in fatty acid metabolism. Soraphen A, a macrocyclic polyketide natural product, is a nanomolar inhibitor against the biotin carboxylase (BC) domain of human, yeast, and other eukaryotic ACCs. Here we report the crystal structures of the yeast BC domain, alone and in complex with soraphen A. Soraphen has extensive interactions with an allosteric site, about 25 Å from the active site. The specificity of soraphen is explained by large structural differences between the eukaryotic and prokaryotic BC in its binding site, confirmed by our studies on the effects of single-site mutations in this binding site. Unexpectedly, our structures suggest that soraphen may bind in the BC dimer interface and inhibit the BC activity by disrupting the oligomerization of this domain. Observations from native gel electrophoresis confirm this structural insight. The structural information provides a foundation for structure-based design of new inhibitors against these enzymes.

Introduction

The obesity epidemic is a serious health threat in the U.S. and in many other countries around the world (Friedman, 2003; Hill et al., 2003). Roughly one-third of the population in the U.S. are obese, and another one-third are overweight. Most significantly, obesity often predisposes the affected individuals to other serious diseases, such as type 2 diabetes and cardiovascular diseases. However, there is currently a lack of effective therapeutic agents for the treatment of this epidemic.

Acetyl-coenzyme A carboxylases (ACCs) have crucial roles in the metabolism of fatty acids and, therefore, are important targets for drug development against obesity, diabetes, and other diseases (Abu-Elheiga et al., 2001; Alberts and Vagelos, 1972; Cronan and Waldrop, 2002; Harwood et al., 2003; Wakil et al., 1983; Zhang et al., 2003, 2004a, 2004b). ACCs catalyze the carboxylation of acetyl-CoA to produce malonyl-CoA. In mammals, ACC1 is present in the cytosol of liver and adipose tissues and controls the committed step in the biosynthesis of long-chain fatty acids (Wakil et al., 1983). In comparison, ACC2 is associated with the outer membrane of mitochondria in the heart and muscle. Its malonyl-CoA product is a potent inhibitor of carnitine palmitoyltransferase I, which facilitates the transport of long-chain acyl-CoAs into the mitochondria for oxidation (McGarry and Brown, 1997; Ramsay et al., 2001). The importance of ACCs for drug discovery is underscored by the observations that mice lacking ACC2 have elevated fatty acid oxidation, reduced body fat, and reduced body weight (Abu-Elheiga et al., 2001, 2003; Lenhard and Gottschalk, 2002).

Eukaryotic ACCs are large, single-chain, multidomain enzymes, with a biotin carboxylase (BC) domain, a biotin carboxyl carrier protein (BCCP) domain, and a carboxyltransferase (CT) domain, whereas these activities exist as separate subunits in the prokaryotic ACCs (Figure 1A) (Abu-Elheiga et al., 2001; Lenhard and Gottschalk, 2002; Wakil et al., 1983). The BC activity catalyzes the ATP-dependent carboxylation of biotin (Figure 1B), and the CT activity catalyzes the transfer of the activated carboxyl group to acetyl-CoA to produce malonyl-CoA. The amino acid sequences of the BC domains are highly conserved among the eukaryotes, with 63% sequence identity between those of yeast ACC and human ACC1 (Figure 1C). In contrast, the sequence conservation between the eukaryotic and prokaryotic BC is much weaker. For example, there is only 35% amino acid identity between yeast and *E. coli* BC (Figure 1C). Moreover, the yeast BC domain, with 570 residues, is ~120 residues larger than the *E. coli* BC subunit (Figure 1A).

Soraphen A was originally isolated from the culture broth of *Sorangium cellulosum*, a soil-dwelling myxobacterium, for its potent antifungal activity (Gerth et al., 1994, 2003). This polyketide natural product contains an unsaturated 18-membered lactone ring, an extracyclic phenyl ring, 2 hydroxyl groups, 3 methyl groups, and 3 methoxy groups (Bedorf et al., 1993; Ligon et al., 2002) (Figure 2A). There is also a 6-membered ring within the macrocycle formed by a hemiketal between the C3 carbonyl and C7 hydroxyl (Figure 2A). Soraphen A has demonstrated strong promise as a broad-spectrum fungicide against various plant pathogenic fungi (Pridzun et al., 1995). Genetic and biochemical studies show that soraphen A is a potent inhibitor of eukaryotic ACCs, and specifically their BC domains (Gerth et al., 1994, 2003; Pridzun, 1991, 1995; Vahlensieck and Hinnen, 1997; Vahlensieck et al., 1994), with K_d values of about 1 nM (Behrbohm, 1996; Weatherly et al., 2004). In comparison, the compound has no effect on bacterial BC subunits (Behrbohm, 1996; Weatherly et al., 2004). However, it is not known how soraphen A achieves its activity and its specificity toward the eukaryotic ACCs.

To reveal the molecular mechanism for the potent inhibitory activity of this natural product against the eukaryotic ACCs, we have determined the crystal structure of the yeast BC domain in complex with soraphen A at 1.8 Å resolution. The structure reveals extensive interactions between soraphen and the BC domain, explaining its strong affinity. Large structural differences between the eukaryotic and bacterial BC in the soraphen binding site precludes the binding of soraphen to the

*Correspondence: tong@como.bio.columbia.edu

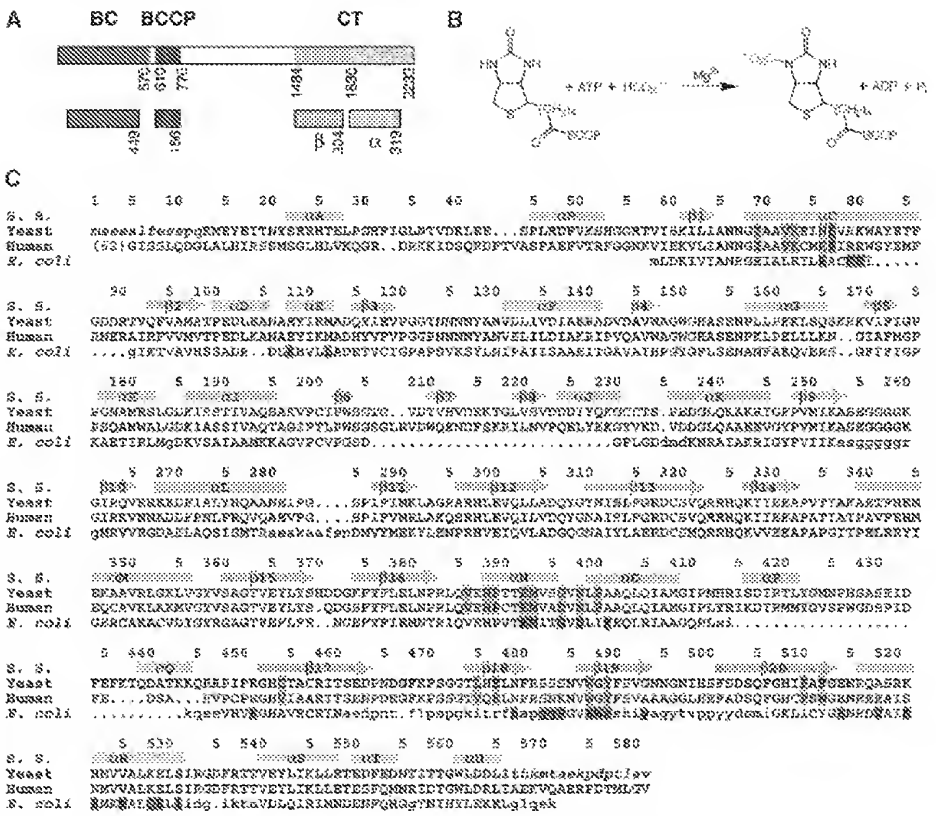

Figure 1. The Biotin Carboxylase Domain of Acetyl Coenzyme-A Carboxylase

(A) Domain organization of yeast ACC (top) and the subunits of *E. coli* ACC (bottom). BC, biotin carboxylase; BCCP, biotin carboxyl carrier protein; CT, carboxyltransferase.

(B) The reaction catalyzed by the BC activity.

(C) Sequence alignment of the BC domains of yeast ACC and human ACC1, and the BC subunit of *E. coli* ACC. Residues involved in binding soraphen are highlighted in green, and in red for Ser77. Residues in the dimer interface of *E. coli* BC are highlighted in magenta. Residues in bacterial BC that are structurally equivalent to those in yeast BC are shown in upper case. S.S., secondary structure.

bacterial enzymes. Our structures suggest soraphen inhibits the BC domain by an unexpected mechanism. It may bind in the dimer interface, thereby disrupting the oligomerization of this domain, which is crucial for its catalytic activity. The structural observation is supported by our native gel electrophoresis experiments. We have developed a fluorescence-based binding assay, which allowed us to characterize the effects of single-site mutations in the soraphen binding site on inhibitor sensitivity.

Results and Discussion

Structure Determination

The crystal structure of the BC domain of yeast ACC in complex with soraphen A was determined at 2.9 Å resolution by the seleno-methionyl multiwavelength anomalous diffraction (MAD) technique (Hendrickson, 1991). These seleno-methionyl crystals actually diffracted to much higher resolutions at the beginning of the experiment, but they suffered serious radiation damage during the data collection. Good quality diffraction lasted only about 5 hr in the X-ray beam, and the exposure time per frame was drastically reduced in order to collect a complete three-wavelength MAD data set in this time. This restricted the diffraction limit of the data set to 2.9 Å resolution.

The positions of the Se atoms and the phases of the reflections were determined from the MAD data with the program Solve (Terwilliger and Berendzen, 1999), and the noncrystallographic symmetry (NCS) relationships among the three molecules of the BC domain in the crystallographic asymmetric unit were determined based on the resulting atomic model. The phase information was transferred to a data set to 1.8 Å resolution collected on a native crystal (Table 1), and NCS averaging using the program DM (CCP4, 1994) was used to improve and extend the phases. The electron density map at 1.8 Å resolution was of excellent quality, and most of the atomic model was built automatically (Terwilliger and Berendzen, 1999).

Interestingly, several attempts at solving the structure using the single-wavelength anomalous diffraction (SAD) method were not successful, as it was not possible to locate the Se atoms based on the SAD data. After the structure was solved by the MAD method, the Se

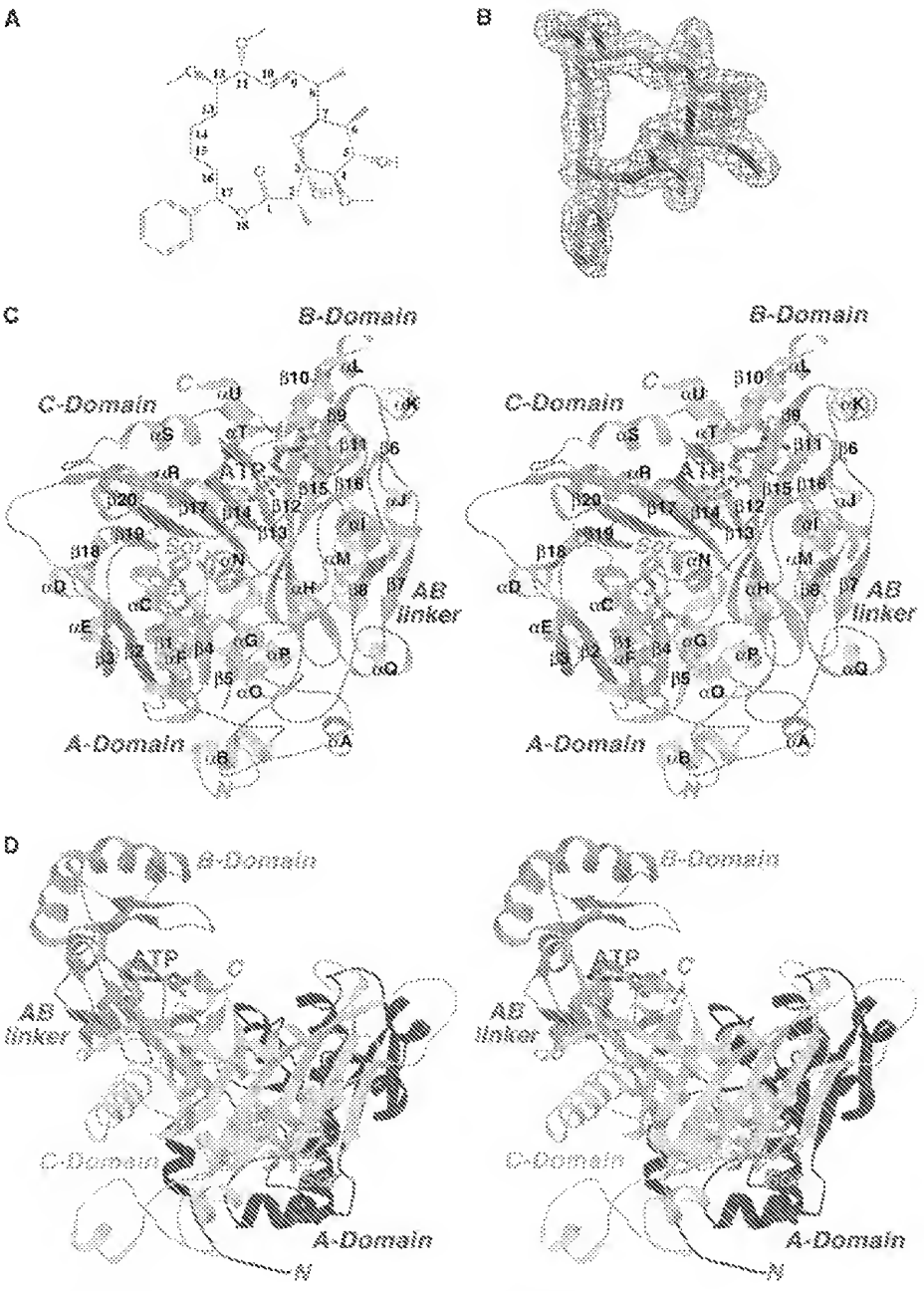

Figure 2. Structure of Biotin Carboxylase in Complex with Soraphen A

(A) Chemical structure of soraphen A. The numbering scheme of atoms in the macrocycle is shown.

(B) Final $2F_o - F_c$ electron density at 1.8 Å resolution for soraphen A, contoured at 1σ. Produced with Setor (Evans, 1993).

(C) Schematic drawing of the structure of yeast BC domain in complex with soraphen A. Residues 535–538 (in the αR-αS loop) are disordered in this molecule and are shown in gray. Soraphen A is shown as a stick model in green for carbon atoms, labeled Sor. The expected position of ATP, as observed in the *E. coli* BC subunit (Thoden et al., 2000), is shown in gray.

(D) Side view of the structure of the BC:soraphen complex. The different domains are colored differently. (C) and (D) were produced with Ribbons (Carson, 1987).

atoms could be positioned with anomalous difference electron density maps using the SAD data. However, these Se sites appeared to have weaker peak heights in the difference maps, which might explain the difficulty in locating them from Patterson or direct methods.

The BC domain of yeast ACC shares 35% amino acid sequence identity with the BC subunit of *E. coli* (Figure 1C), for which crystal structures are available (Thoden et al., 2000; Waldrop et al., 1994). Attempts at solving the structure of the yeast BC domain by molecular re-

Table 1. Summary of Crystallographic Information

Structure	BC:Soraphen A Complex	BC Free Enzyme
Resolution range (Å)	30–1.8	30–2.5
Number of observations	564,576	110,250
R_{merge}[a] (%)	6.9 (32.5)	8.0 (25.1)
I/σ	19.1 (3.0)	16.4 (3.6)
Observation redundancy	3.6 (3.0)	3.7 (3.4)
Number of reflections	150,099	24,971
Completeness (%)	96 (88)	84 (57)
R factor[b] (%)	19.5 (25.8)	25.4 (25.9)
Free R factor[b] (%)	23.0 (28.3)	32.3 (29.7)
Rms deviation in bond lengths (Å)	0.005	0.007
Rms deviation in bond angles (°)	1.2	1.3

[a] $R_{merge} = \sum_h \sum_i |I_{hi} - \langle I_h \rangle| / \sum_h \sum_i I_{hi}$. The numbers in parentheses are for the highest resolution shell.
[b] $R = \sum_h |F_h^o - F_h^c| / \sum_h F_h^o$.

placement were not successful either, which is likely due to the large structural differences between the two enzymes (see below).

The three BC domain molecules in the asymmetric unit do not form dimeric or trimeric association in the crystal, consistent with our light-scattering studies showing that the BC domain is monomeric in solution. Two of the BC domains have essentially the same conformation, with rms distance of 0.4 Å between their equivalent Cα atoms. The third BC domain shows recognizable conformational differences for several loops on the surface of the enzyme, but these are not in the soraphen binding site. Soraphen A has the same binding mode in the three copies of the BC-soraphen complexes in the asymmetric unit.

The Overall Structure

The crystal structure of the BC domain of yeast ACC in complex with soraphen A has been determined at 1.8 Å resolution. The current atomic model has an R factor of 19.5% (Table 1). The bound conformation of soraphen A is clearly defined by the crystallographic analysis (Figure 2B). The majority of the residues (91.6%) are in the most favored region, while none of the residues are in the disallowed region, of the Ramachandran plot (data not shown). The atomic coordinates have been deposited at the Protein Data Bank (accession codes 1W93 and 1W96).

The structure of the yeast BC domain contains 20 β strands (named β1–β20) and 21 α helices (αA–αU) (Figure 2C). The overall structure of the BC domain has the ATP-grasp fold (Artymiuk et al., 1996; Galperin and Koonin, 1997) and consists of three subdomains (Figure 2D) (Thoden et al., 2000; Waldrop et al., 1994). The A-domain covers residues 1–175 (strands β1–β5, helices αA–αG) and has the Rossmann fold, with a central five-stranded fully parallel β sheet. The B-domain (residues 234–293, with β9–β11, αK, and αL) contains a three-stranded antiparallel β sheet with two helices (Figure 2D). A small strand (β6) from the AB linker (residues 176–233, with β6–β8, αH–αJ) extends this β sheet to four strands (Figure 2C). The C-domain (residues 294–566) contains a nine-stranded antiparallel β sheet (β12–β20), with helices (αM–αU) on both sides (Figure 2C).

The B-domain of the *E. coli* BC subunit undergoes a large conformational change upon ATP binding (Thoden et al., 2000), and assumes a closed conformation. The B-domain of yeast BC in the soraphen complex is mostly in the closed conformation, even though ATP is not bound in the active site (Figure 2C).

The Binding Mode of Soraphen

Our structure demonstrates that soraphen A is an allosteric inhibitor of the BC domain, as it is located 25 Å away from the putative position of the ATP molecule in the active site, on the opposite surface of the enzyme (Figure 2D). The A-domain, C-domain, and AB-linker form a cylindrical structure, with the ATP and soraphen molecules located on opposite ends of this cylinder, while the B-domain is a lid on the cylinder (Figure 2D). The structural observation is consistent with kinetic data showing that soraphen A is generally noncompetitive with respect to the substrates of ACC (Behrbohm, 1996).

There are extensive interactions between soraphen A and the BC domain (Figure 3A), explaining the nanomolar binding affinity of this natural product. In addition, most of the residues that are involved in binding soraphen A are highly conserved among the BC domains of eukaryotic ACCs (Figure 1C), consistent with the potent activity of this compound against all of them. For example, the K_d of soraphen for the BC domains of human ACC1 and ACC2 is ~1 nM (unpublished data). The potent activity and the strong sequence conservation between the yeast and human BC domains suggest that soraphen should have the same binding mode to the human BC domains.

Soraphen A is bound at the interface between the A-domain and C-domain (Figure 3A), having interactions with residues in strands β17–β20 and helices αN, αO in the C-domain, as well as several critical residues from helix αC in the A-domain (Figure 3B). One wall of the binding site is formed by strands β17–β20 in the second half of the C-domain (Figure 3A). From the αC helix in the A-domain, residues Lys73 and Arg76, in ion-pair interactions with Glu392 (αN) and Glu477 (β18) in the C-domain, respectively, mediate the binding of soraphen A as well as the interactions between the two domains (Figure 3A). The oxygens of the methoxy groups on C11 and C12 of soraphen are hydrogen bonded to the side chain of Arg76 (αC) (Figure 3B). In addition, Ser77 in helix αC is in direct contact with soraphen A, hydrogen bonded to its C5 hydroxyl group (Figure 3B).

The bound conformation of soraphen A is essentially the same as that of the compound alone (Bedorf et al., 1993), with the exception of a torsional adjustment of the methoxy group on C12. The macrocycle of the compound is placed on the surface of the BC domain (Figure 3C), and 300 Å^2 of the surface area of the BC domain are shielded from the solvent in the complex. The four methylene groups (C13–C16) and the extracyclic phenyl ring of soraphen A are located in a highly hydrophobic environment, and the side chains of Met393 (αN) and Trp487 (β19) make critical contributions to this binding site. The methoxy group on C12 is located in a small pocket on the surface of the enzyme (Figure 3C). Interestingly, our structure suggests that small, hydrophobic

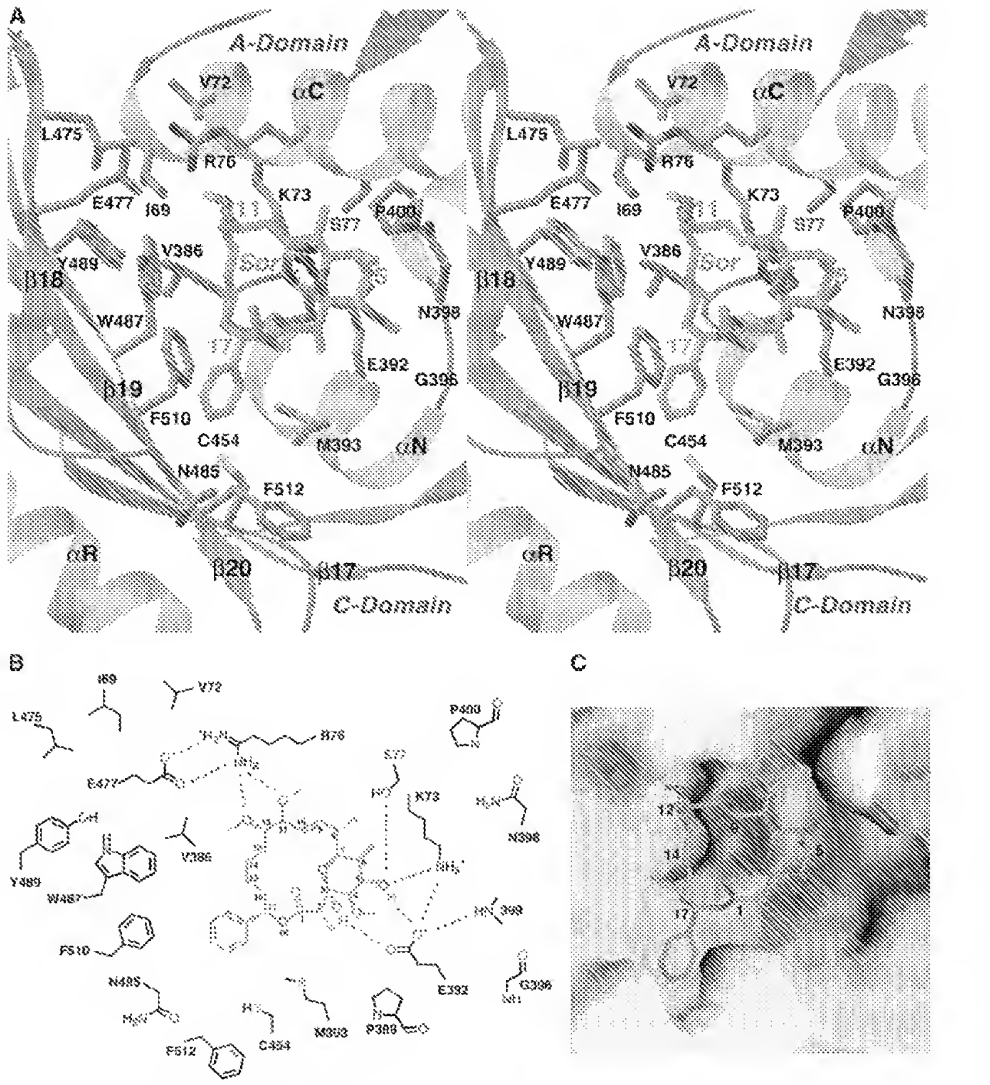

Figure 3. The Binding Mode of Soraphen A

(A) Stereographic drawing showing the binding site for soraphen A. Produced with Ribbons (Carson, 1987).

(B) Schematic drawing of the interactions between soraphen A and the BC domain.

(C) Molecular surface of the BC domain in the soraphen binding site. Produced with Grasp (Nicholls et al., 1991).

substituents at C13 or C14 might be able to have favorable interactions with a neighboring pocket (Figure 3C).

The observed binding mode of soraphen A is supported by biochemical observations and explains the molecular basis for resistance mutations. Most importantly, it has been found that mutation of Ser77 of yeast ACC to Tyr renders the enzyme resistant to soraphen A (Vahlensieck and Hinnen, 1997; Vahlensieck et al., 1994). Based on our structure, this mutation will introduce steric clash between the Tyr side chain and soraphen (Figure 3A), thereby disallowing the binding of the compound. The K73R mutation has also been found to confer resistance to soraphen A (Vahlensieck and Hinnen, 1997). The structure suggests that this mutation may disrupt the ion-pair with Glu392, which should be detrimental for the binding of the compound as well (Figure 3A). Our additional studies show that mutation of other residues in this binding site can also disrupt soraphen binding (see below).

The observed binding mode of soraphen A can also explain the structure-activity relationship (SAR) that has been observed for analogs of this natural product. Our structure of the complex shows that the entire macrocycle of soraphen is involved in binding to the BC domain, consistent with the SAR that substructures of soraphen do not have antifungal activities (Loubinoux et al., 1995a, 1995b, 1995c, 1995d). Changing the stereochemistry of the phenyl substituent at C17 abolished the activity of the compound, while replacing the phenyl ring with other groups led to a reduction in activity (Schummer et al., 1995). The *trans* double bond between C9 and C10 does not have specific interactions with the enzyme (Figure

3A), and it can be reduced (producing soraphen F) with only a moderate loss of activity (Hofle et al., 1995). Interestingly, removing the hydroxyl group on C5 only produces a 5-fold loss of activity (Kiffe et al., 1997), suggesting that the hydrogen bond to Ser77 may not be crucial for the activity of soraphen A (Figure 3B).

Molecular Basis for the Specificity of Soraphen

To understand the molecular basis for the specificity of soraphen A for eukaryotic BC domains, we compared the structures of the yeast BC domain and bacterial BC subunit (Thoden et al., 2000; Waldrop et al., 1994). Despite sharing 35% amino acid sequence identity, there are significant differences between the two structures (Figures 2C and 4A). Only 364 of the 447 Cα atoms of the *E. coli* BC structure can be superimposed to within 3 Å of the yeast BC structure (Figure 1C), and the rms distance for these equivalent Cα atoms is 1.6 Å. Compared to the bacterial BC subunit, the eukaryotic BC domain has insertions in the A-domain (αA and αB at the N terminus), AB linker (β7, β8, and αJ), and C-domain (αP and αQ) (Figure 4A), explaining its larger size.

The largest structural differences between the eukaryotic and bacterial BC are seen in the second half of the C-domain, which is also the binding site for soraphen. The position of strand β19 in bacterial BC shifts by about 3 Å toward the soraphen molecule, and strand β18 is absent in the *E. coli* BC structure (Figure 4B). As a consequence, the molecular surface of bacterial BC subunit is incompatible with soraphen A binding (Figure 4C), and there is serious steric clash between soraphen and residues in strand β19 of the bacterial BC structure. In addition to these differences in main chain conformations, changes in amino acid side chains in this binding site are also detrimental for soraphen binding to the bacterial BC subunit (see below). Overall, structural and amino acid sequence differences between the bacterial and eukaryotic BC determine the specificity of soraphen for eukaryotic ACCs.

A Fluorescence-Based Binding Assay

We next developed a fluorescence-based binding assay using the structural information. Our structures show that Trp487 is mostly exposed to the solvent in the free enzyme but is buried by soraphen A in the complex (Figure 3A). This suggests that the fluorescence emission of this residue should be enhanced in the complex, which enabled us to establish the fluorescence binding assay (Figure 4D). There is also a slight blue shift in the fluorescence emission maximum upon soraphen binding. The observed increase in Trp fluorescence as a function of soraphen concentration can be easily fit to a one-site binding model (Figure 4D), confirming that there is a single binding site for soraphen in the BC domain. The binding affinity obtained from this fluorescence assay is generally in good agreement with that based on the radioactive binding assay (Table 2) (Weatherly et al., 2004). Compared to the radioactive assay, the fluorescence assay has the advantage that it can measure affinity between 1 nM and 10 μM, whereas the radioactive assay is limited to K_d values below ~50 nM.

The establishment of this fluorescence binding assay allowed us to further characterize the soraphen binding site. We selected those residues in this region that show differences to their equivalents in the *E. coli* BC subunit, and introduced these changes to yeast BC domain as single-site mutations. The mutants were expressed and purified following the same protocol as the wild-type enzyme. They migrated as monomers on a gel-filtration column (data not shown), suggesting that the mutations have not disturbed the overall structure of the BC domain. These mutants generally have drastically reduced affinity for soraphen (Table 2), confirming the structural information and suggesting another molecular mechanism for the specificity of soraphen for the BC domains of eukaryotic ACCs. The K73R mutant has a 500-fold loss in affinity for soraphen, such that the K_d is now in the micromolar range (Table 2). At the same time, the conservative F510I mutation has only a minor impact on the affinity for soraphen (Table 2).

Finally, there is little fluorescence change for the W487R mutant in the presence of soraphen (data not shown), confirming that the fluorescence increase observed for the wild-type enzyme and the other mutants is due almost exclusively to the Trp487 residue.

Soraphen Binding Causes Only Small Conformational Changes in the BC Domain

What is the molecular mechanism for the potent inhibitory activity of soraphen A? One possibility is that soraphen A allosterically interferes with either substrate binding or catalysis in the active site. However, based on our structures and the current biochemical information, this is unlikely to be the case.

To assess whether there are conformational changes in the BC domain upon soraphen binding, we have determined the crystal structure of the free enzyme of yeast BC domain at 2.5 Å resolution (Table 1). The overall structure of the free enzyme is the same as that of the soraphen complex (see Supplemental Figure S1A at http://www.molecule.org/cgi/content/full/16/6/881/DC1/), and the rms distance for all the equivalent Cα atoms of the two structures is 0.6 Å. In addition, there are only small changes in the soraphen binding site (Supplemental Figure S1B) and the active site. This suggests that soraphen binding does not induce an overall conformational change in the BC domain, making an allosteric effect on the active site by soraphen unlikely.

The structural observation is also supported by our preliminary experiments showing that soraphen A does not interfere with the binding of a fluorescent ATP analog (Mant-ATP) to the active site of yeast BC domain (unpublished data). Interestingly, the B-domain assumes the closed conformation in the yeast BC domain, even in the absence of ATP (Supplemental Figure S1A), in sharp contrast to observations from the structure of bacterial BC subunit (Kondo et al., 2004; Thoden et al., 2000; Waldrop et al., 1994).

Soraphen May Be a Protein-Protein Interaction Inhibitor

Our structural information suggests instead that soraphen A may have a different mechanism of action. This natural product may function as a protein-protein interaction inhibitor, and abolishes the activity of the BC domain by disrupting its dimerization or oligomerization.

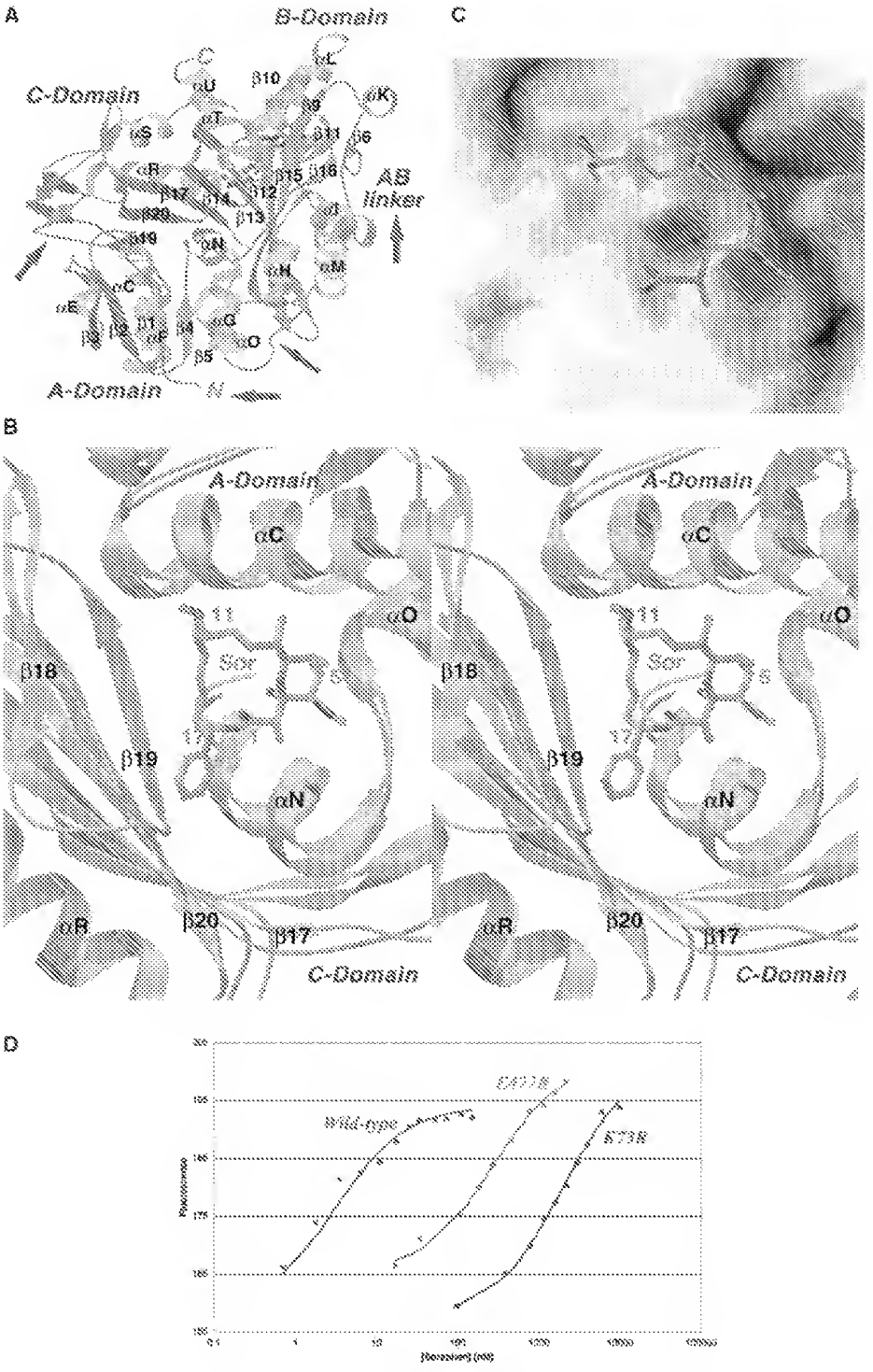

Figure 4. Conformational Differences in the Bacterial BC Subunit Precludes Soraphen Binding

(A and B) (A) Schematic drawing of the structure of *E. coli* BC subunit in complex with ATP (Thoden et al., 2000). Regions of large structural differences to the yeast BC domain are indicated with red arrows. (B) Structural comparison between yeast (in yellow) and *E. coli* (cyan) BC in the soraphen binding site. (A) and (B) were produced with Ribbons (Carson, 1987).

(C) Molecular surface of the *E. coli* BC in the soraphen binding site. The soraphen molecule is shown for reference and has extensive steric clash with the bacterial BC. Produced with Grasp (Nicholls et al., 1991).

(D) Fluorescence-based assay for soraphen binding to the BC domain. Trp emission at 340 nm for the wild-type, K73R, and E477R mutants is plotted as a function of the soraphen concentration. The curves represent fits to a one-site binding model.

Table 2. Affinity of Soraphen for Wild-Type and Mutant Yeast BC Domains

Yeast BC Domain	K_d (nM) (Radioactive Assay)	K_d (nM) (Fluorescence Assay)
Wild-type	2.0 ± 0.9	3.9 ± 0.7
I69E	—[a]	104 ± 18
K73R	—[b]	2006 ± 174
S77Y	—[b]	n.d.[c]
E477R	24.7 ± 10.4	274 ± 30
N485G	2.7 ± 0.4	55 ± 4
W487R	—[a]	n.d.[c]
F510I	5.7 ± 1.0	10.6 ± 4.8

[a] Detectable specific binding observed at up to 60 nM soraphen A (with 10 nM protein), but insufficient data for K_d determination
[b] No specific binding observed at up to 60 nM soraphen A (with 10 nM protein)
[c] n.d., not done

The BC subunits of bacterial ACCs are dimeric enzymes (Figure 5A) (Thoden et al., 2000; Waldrop et al., 1994), and dimerization is essential for their activity (Janiyani et al., 2001). Similarly, yeast ACC is believed to function as a dimer or oligomer, while the isolated BC domain is monomeric in solution and is catalytically inactive (Weatherly et al., 2004). The surface area of yeast BC domain that mediates the binding of soraphen A is equivalent to the dimer interface of the bacterial BC subunits (Figures 1C and 5A), and it is likely that the eukaryotic BC domains employ a similar mode of dimerization. Therefore, soraphen binding is expected to disrupt the dimerization of the BC domains, thereby leading to their inhibition.

However, the exact molecular mechanism for the dimerization dependence of the activity of BC is currently not clear, as the two active sites of the BC dimer are located far from the dimer interface (Figure 5A). Studies with the bacterial BC subunits show that if the active site of one of the two monomers of the dimer is disabled (by mutation), the resulting heterodimer does not exhibit any catalytic activity (Janiyani et al., 2001). This indicates that there is communication between the two active sites, and hence the requirement for the dimerization of the enzyme. A similar situation may exist for the dimers of eukaryotic BC domains. Interestingly, the structure of the active site of the isolated yeast BC domain is similar to that of the bacterial BC subunits. This suggests that dimerization may not be required to form the correct organization of the active site of the yeast BC domain.

To obtain experimental evidence for the effects of soraphen A on the oligomerization state of BC domains, we examined the mobility of the yeast BC domain in a native gel electrophoresis assay. Similar observations were made using the BC domains of human ACC1 and *Ustilago maydis* ACC (data not shown) (Weatherly et

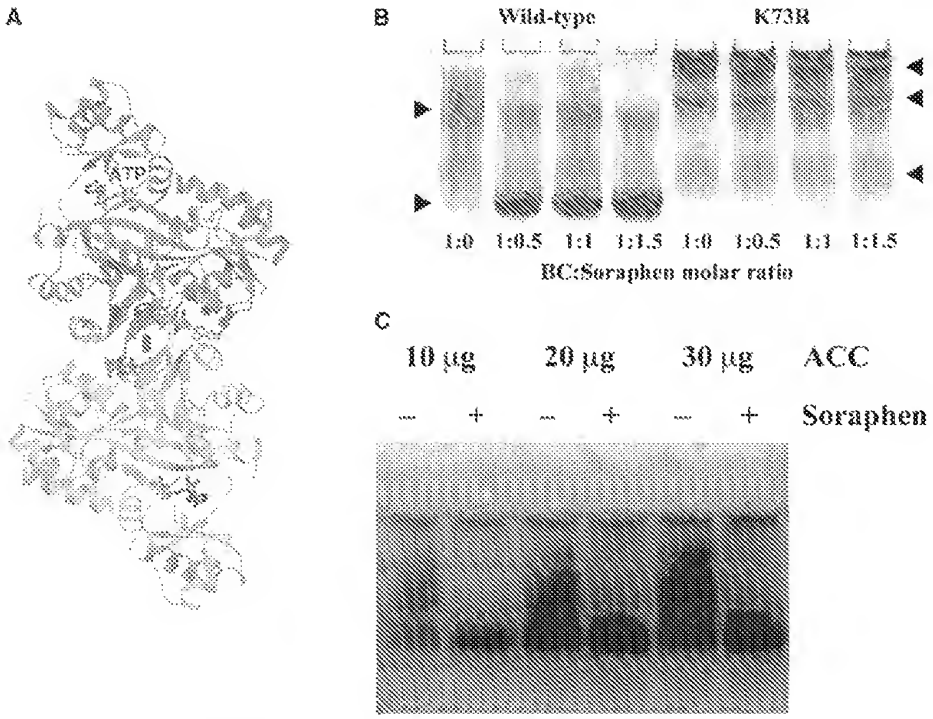

Figure 5. Soraphen A May Disrupt the Oligomerization of the BC Domain

(A) Schematic drawing of the dimer of *E. coli* BC subunit in complex with ATP (Thoden et al., 2000). The dimer axis is indicated with the magenta oval. The position of soraphen as observed in the yeast BC domain structure is shown for reference.

(B) Native gel (12%) showing the electrophoretic mobility of wild-type and K73R mutant of yeast BC domain in the absence or presence of soraphen. Possible bands in the gel are marked with the arrowheads. Each lane was loaded with 20 μg of protein in 8 μl.

(C) Native gel (4%–20% gradient) showing the electrophoretic mobility of wild-type full-length *Ustilago maydis* ACC in the absence or presence of 10-fold molar excess of soraphen.

al., 2004). In the absence of soraphen A, wild-type BC domain runs as several smeared bands on the gel, suggesting various states of oligomerization (Figure 5B). In the presence of soraphen A, a sharp band is observed, with the fastest migrating speed (Figure 5B). Increasing the molar ratio between soraphen and the BC domain converts more of the protein into this fast-migrating species (Figure 5B). Based on our structural information, it is highly likely that this sharp band corresponds to the BC:soraphen complex, in a monomeric state, whereas the smeared bands with reduced mobility correspond to dimeric or oligomeric states of the enzyme (Figure 5B). As a control, the mobility of the K73R mutant of the BC domain, which has drastically reduced affinity for soraphen (Table 2), is not affected by the presence of soraphen A (Figure 5B). At the same time, the affinity for self-association of the isolated BC domain is likely to be low, as we observed only monomers in gel filtration and solution light scattering experiments (data not shown). It is likely that the BC domain can achieve a higher local concentration in the native gel enviroment, enabling its oligomerization in the absence of soraphen (Figure 5B).

To obtain further support for the proposed mechanism of action of soraphen A, we examined its effects on the oligomerization states of full-length ACC from *Ustilago maydis* (Weatherly et al., 2004). The results show that the presence of soraphen can also change the migration behavior of the full-length enzyme in the native gel, such that a smear in the absence of the compound (possibly corresponding to oligomers) collapses down to a single band in its presence (Figure 5C). This is consistent with our inhibition mechanism, and suggests that dimerization of the BC domain might also be important for the oligomerization of full-length ACCs. (In contrast to the mammalian ACCs, the fungal ACCs do not require citrate for oligomerization.) Our further studies with BC domains fused with GST as well as tethered BC dimers also showed similar effects of soraphen on the native gel migration behavior of these proteins (see Supplemental Figures S2 and S3).

ACCs are attractive targets for the development of new therapeutic agents against obesity, diabetes, and many other serious diseases. The eukaryotic ACCs possess two catalytic activities, embodied in the BC and the CT domains (Figure 1A). Potent, small-molecule inhibitors have been successfully identified and developed against the CT domain of this enzyme. For example, two classes of compounds have been used commercially as herbicides for more than 30 years (Delye et al., 2003; Devine and Shukla, 2000; Gronwald, 1991; Zagnitko et al., 2001), both of which inhibit the CT domains of the ACC enzyme from sensitive plants (Rendina et al., 1988; Zhang et al., 2004b). More recently, potent inhibitors of mammalian ACCs have been identified by high-throughput screening (Harwood et al., 2003), and kinetic and structural studies confirm that these compounds also function at the active site of the CT domain (Harwood et al., 2003; Zhang et al., 2004a). Moiramide has recently been reported as a potent allosteric inhibitor of the CT subunits of bacterial ACCs (Freiberg et al., 2004). Up till now, soraphen is the only known potent inhibitor of the BC domain of eukaryotic ACCs. Its potent fungicidal activity demonstrates that inhibitors against the BC domain could also prove efficacious in the treatment of diseases linked to ACCs, opening a new avenue of discovery in the identification of inhibitors against these enzymes.

Besides the ACCs, there are three other biotin-dependent enzymes in mammals. The amino acid sequence conservation between their BC domains and the BC domains of ACCs is rather limited, between 25% and 40% sequence identity. In addition, our studies show that soraphen does not bind in the active site, and the sequence conservation for its binding site is even lower. In fact, residues that interact with soraphen in the ACCs are not conserved in the other biotin enzymes. This is strongly supported by published results showing that soraphen does not inhibit the activity of the biotin-dependent enzyme pyruvate carboxylase (Pridzun et al., 1995).

Polyketide natural products have become highly successful antibiotics, antivirals, antitumor agents, and immunosuppressants (Cane, 1997; Cane et al., 1998; Walsh, 2004). Our structural and biochemical studies reveal the molecular mechanism for the potent inhibitory activity of the polyketide soraphen A. The compound binds in the dimer interface and is a potent inhibitor of protein-protein interactions. The structural information should help the design and development of new soraphen analogs, with improved pharmacokinetic properties and reduced toxicity profiles, which may enable this natural product to become a broad-spectrum fungicide. The potent activity of this compound against human ACCs suggests the intriguing possibility that this natural product could also lead to compounds that are efficacious against obesity and diabetes.

Experimental Procedures

Protein Expression and Purification

The expression and purification of the yeast BC domain followed the protocols that we have described for the *Ustilago* BC domain (Weatherly et al., 2004). Residues 2–581 of yeast ACC were subcloned into the pET28a vector (Novagen) and overexpressed in *E. coli* BL21(DE3) Rosetta cells (Novagen) at 20 C. The soluble protein was purified by nickel agarose, anion exchange, and gel-filtration chromatography. The purified BC domain was concentrated to 60 mg/ml in a buffer containing 100 mM Tris (pH 8.5), 100 mM NaCl, 5% (v/v) glycerol, and 5 mM DTT. The recombinant protein contains an N-terminal hexa-histidine tag, together with about 30 other residues from the expression vector. These residues were not removed for crystallization.

The selenomethionyl protein was produced in B834(DE3) cells (Novagen), grown in defined LeMaster media supplemented with selenomethionine (Hendrickson et al., 1990), and purified following the same protocol as that for the native protein. The selenomethionyl protein was concentrated to 50 mg/ml in a solution of 100 mM Tris (pH 8.5), 150 mM NaCl, 5% (v/v) glycerol, and 8 mM DTT.

Protein Crystallization

Crystals of yeast BC domain in complex with soraphen A were obtained at 22°C by the sitting-drop vapor diffusion method. The protein at 50 mg/ml was incubated with 0.88 mM soraphen A (protein:inhibitor molar ratio of 1:1.2) at 4°C for 1 hr prior to crystallization. The reservoir solution contains 100 mM Bis-Tris (pH 6.0), 26% (w/v) PEG3350, 200 mM NaCl, and 400 mM $MgCl_2$. The crystals grew to full size in about 12–18 days, and microseeding was necessary to obtain crystals of diffraction quality. The crystals were cryo-protected by transferring to the reservoir solution supplemented with 9% glycerol and flash-frozen in liquid propane for data collection at 100 K. They belong to space group $P2_1$, with cell parameters of

a = 63.83 Å, b = 96.52 Å, c = 139.95 Å, and β = 96.82°. There are three copies of the BC:soraphen complex in the asymmetric unit.

Crystals of the selenomethionyl protein in complex with soraphen A were grown with the sitting-drop vapor diffusion method at 22°C. The reservoir solution contained 100 mM Bis-Tris (pH 5.8), 25% (w/v) PEG3350, 100 mM NaCl, 200 mM $MgCl_2$, 8% glycerol, and 2 mM DTT. Microseeding from the native crystals was essential. The crystals are isomorphous to those of the native protein.

Crystals of the free enzyme of yeast BC domain were obtained by sitting-drop vapor diffusion method at 4°C. The reservoir solution contained 100 mM Bis-Tris propane (pH 6.0), 23% (w/v) PEG3350, 200 mM NaCl, 400 mM $MgCl_2$, and 5% glycerol. The crystals belong to space group $P6_2$, with cell parameters of a = b = 101.74 Å, and c = 145.83 Å. There is one molecule of the BC domain in the asymmetric unit. Crystallographic analysis suggests that the crystal is almost perfectly merohedrally twinned, as the diffraction data display 6/mmm symmetry.

Structure Determination

X-ray diffraction data were collected at the X4A beamline of the National Synchrotron Light Source (NSLS). The diffraction images were processed with the HKL package (Otwinowski and Minor, 1997). A selenomethionyl multiwavelength anomalous diffraction (MAD) data set to 2.9 Å resolution and a native data set to 1.8 Å resolution were collected. The MAD data were loaded into the program Solve (Terwilliger and Berendzen, 1999), which located the Se sites, phased the reflections, and built partial models for three molecules of the BC domain.

The noncrystallographic symmetry (NCS) parameters were determined based on the partial models, and the reflection phases were transferred to the native data set. The phase information was extended to 1.8 Å resolution by NCS averaging with the program DM (CCP4, 1994), and Solve was able to automatically build in 60% of the residues into this map. Additional residues were built manually with the program O (Jones et al., 1991). The structure refinement was carried out with the program CNS (Brunger et al., 1998). Residues 248 and 333 are modeled as *cis* prolines, and their equivalents in *E. coli* BC are also in the *cis* conformation (Waldrop et al., 1994). The crystallographic information is summarized in Table 1.

The structure of the free enzyme of yeast BC was determined by the molecular replacement method with the program COMO (Jogl et al., 2001). The diffraction data on this crystal had apparent *P6/mmm* symmetry, and the twinning fraction was estimated to be 0.5. Refinement procedures incorporating the twinning could not lower the free R factor. Therefore, the diffraction data set was detwinned based on the atomic model, using standard procedures in the CNS program (Brunger et al., 1998), and structure refinement was performed against this modified data set. As the model improved, the detwinning was repeated several times against the original observed data.

Mutagenesis and Binding Assays

The mutants were designed based on the structural information and made with the QuikChange kit (Stratagene). The mutants were sequenced, expressed in *E. coli*, and purified following the same protocol as that for the wild-type BC domain. The affinity of soraphen for the mutants were assessed using a radioactive binding assay (Weatherly et al., 2004).

We have developed a fluorescence-based binding assay using our structural information, which monitored the increase in Trp emission upon soraphen binding. The binding buffer initially contained 100 mM Tris (pH 8.0), 100 mM NaCl, and 50 nM wild-type or mutant enzyme, and increasing concentrations of soraphen A was titrated into the solution. The observed binding curve is fitted using conventional methods or the tight binding model where appropriate.

Native Gel Assays

Wild-type yeast BC domain or the K73R mutant (at 5 mg/ml concentration) were incubated with or without soraphen A on ice for 1 hr prior to electrophoresis. For electrophoresis in a 12% polyacrylamide gel (pH 8.8), 4 μl of the protein/inhibitor solution, and 4 μl of the loading buffer (1M Tris [pH 6.8], 20% [v/v] glycerol, and 0.04% [w/v] bromophenol blue) were loaded for each lane. The electrophoresis was performed in a Tris-glycine running buffer under 150 V at 4°C for 5 hr.

Acknowledgments

We thank Randy Abramowitz and Xiaochun Yang for setting up the beamline at X4A; Javed Khan, Xiao Tao, Gerwald Jogl, Hailong Zhang, and Corey Mandel for help with data collection at the synchrotron source; and Professor Gerhard Höfle for providing soraphen A. This research is supported in part by grants from the NIH to L.T. (DK67238) and T.D.E. (1R43DK068962-01).

Received: July 21, 2004
Revised: September 14, 2004
Accepted: October 7, 2004
Published: December 21, 2004

References

Abu-Elheiga, L., Matzuk, M.M., Abo-Hashema, K.A.H., and Wakil, S.J. (2001). Continuous fatty acid oxidation and reduced fat storage in mice lacking acetyl-CoA carboxylase 2. Science *291*, 2613–2616.

Abu-Elheiga, L., Oh, W., Kordari, P., and Wakil, S.J. (2003). Acetyl-CoA carboxylase 2 mutant mice are protected against obesity and diabetes induced by high-fat/high-carbohydrate diets. Proc. Natl. Acad. Sci. USA *100*, 10207–10212.

Alberts, A.W., and Vagelos, P.R. (1972). Acyl-CoA carboxylases. In The Enzymes, P.D. Boyer, ed. (New York: Academic Press), pp. 37–82.

Artymiuk, P.J., Poirrette, A.R., Rice, D.W., and Willett, P. (1996). Biotin carboxylase comes into the fold. Nat. Struct. Biol. *3*, 128–132.

Bedorf, N., Schonburg, D., Gerth, K., Reichenbach, H., and Hofle, G. (1993). Isolation and structure elucidation of soraphen A1alpha, a novel macrolide from Sorangium cellulosum. Liebigs Ann. Chem. *9*, 1017–1021.

Behrbohm, H. (1996). Acetyl-CoA Carboxylase aus Ustilago maydis. Reinigung, Charakterisierung und Intersuchungen zur Inhibierung durch Soraphen A. Ph.D. thesis, Technical University of Braunschweig, Braunschweig, Germany.

Brunger, A.T., Adams, P.D., Clore, G.M., DeLano, W.L., Gros, P., Grosse-Kunstleve, R.W., Jiang, J.-S., Kuszewski, J., Nilges, M., Pannu, N.S., et al. (1998). Crystallography & NMR System: a new software suite for macromolecular structure determination. Acta Crystallogr. D Biol. Crystallogr. *54*, 905–921.

Cane, D.E. (1997). Polyketide and nonribosomal polypeptide biosynthesis. From Collie to Coli. Chem. Rev. *97*, 2463–2464.

Cane, D.E., Walsh, C.T., and Khosla, C. (1998). Harnessing the biosynthetic code: combinations, permutations, and mutations. Science *282*, 63–68.

Carson, M. (1987). Ribbon models of macromolecules. J. Mol. Graph. *5*, 103–106.

CCP4 (Collaborative Computational Project, Number 4) (1994). The CCP4 suite: programs for protein crystallography. Acta Crystallogr. D Biol. Crystallagr. *50*, 760–763.

Cronan, J.E., Jr., and Waldrop, G.L. (2002). Multi-subunit acetyl-CoA carboxylases. Prog. Lipid Res. *41*, 407–435.

Delye, C., Zhang, X.-Q., Chalopin, C., Michel, S., and Powles, S.B. (2003). An isoleucine residue within the carboxyl-transferase domain of multidomain acetyl-coenzyme A carboxylase is a major determinant of sensitivity to aryloxyphenoxypropionate but not to cyclohexanedione inhibitors. Plant Physiol. *132*, 1716–1723.

Devine, M.D., and Shukla, A. (2000). Altered target sites as a mechanism of herbicide resistance. Crop Prot. *19*, 881–889.

Evans, S.V. (1993). SETOR: hardware lighted three-dimensional solid model representations of macromolecules. J. Mol. Graph. *11*, 134–138.

Freiberg, C., Brunner, N.A., Schiffer, G., Lampe, T., Pohlmann, J., Brands, M., Raabe, M., Habich, D., and Ziegelbauer, K. (2004). Identification and characterization of the first class of bacterial acetyl-CoA carboxylase inhibitors with antibacterial activity. J. Biol. Chem. *279*, 26066–26073.

Friedman, J.M. (2003). A war on obesity, not the obese. Science *299*, 856–858.

Galperin, M.Y., and Koonin, E.V. (1997). A diverse superfamily of enzymes with ATP-dependent carboxylase-amine/thiol ligase activity. Protein Sci. *6*, 2639–2643.

Gerth, K., Bedorf, N., Irschik, H., Hofle, G., and Reichenbach, H. (1994). The soraphens: a family of novel antifungal compounds from Sorangium cellulosum (Myxobacteria). I. Soraphen A1 alpha: fermentation, isolation, biological properties. J. Antibiot. (Tokyo) *47*, 23–31.

Gerth, K., Pradella, S., Perlova, O., Beyer, S., and Muller, R. (2003). Myxobacteria: proficient producers of novel natural products with various biological activities-past and future biotechnological aspects with the focus on the genus Sorangium. J. Biotechnol. *106*, 233–253.

Gronwald, J.W. (1991). Lipid biosynthesis inhibitors. Weed Sci. *39*, 435–449.

Harwood, H.J., Jr., Petras, S.F., Shelly, L.D., Zaccaro, L.M., Perry, D.A., Makowski, M.R., Hargrove, D.M., Martin, K.A., Tracey, W.R., Chapman, J.G., et al. (2003). Isozyme-nonselective N-substituted bipiperidylcarboxamide acetyl-CoA carboxylase inhibitors reduce tissue malonyl-CoA concentrations, inhibit fatty acid synthesis, and increase fatty acid oxidation in cultured cells and in experimental animals. J. Biol. Chem. *278*, 37099–37111.

Hendrickson, W.A. (1991). Determination of macromolecular structures from anomalous diffraction of synchrotron radiation. Science *254*, 51–58.

Hendrickson, W.A., Horton, J.R., and LeMaster, D.M. (1990). Selenomethionyl proteins produced for analysis by multiwavelength anomalous diffraction (MAD): a vehicle for direct determination of three-dimensional structure. EMBO J. *9*, 1665–1672.

Hill, J.O., Wyatt, H.R., Reed, G.W., and Peters, J.C. (2003). Obesity and the environment: Where do we go from here? Science *299*, 853–855.

Hofle, G., O'Sullivan, A.C., Rihs, G., Sutter, M., and Winkler, T. (1995). The stereoselective derivatisation of the Re or Si faces of the Δ9,10-double bond of soraphen A. Tetrahedron *51*, 3159–3174.

Janiyani, K., Bordelon, T., Waldrop, G.L., and Cronan, J.E., Jr. (2001). Function of Escherichia coli biotin carboxylase requires catalytic activity of both subunits of the homodimer. J. Biol. Chem. *276*, 29864–29870.

Jogl, G., Tao, X., Xu, Y., and Tong, L. (2001). COMO: a program for combined molecular replacement. Acta Crystallogr. *D57*, 1127–1134.

Jones, T.A., Zou, J.Y., Cowan, S.W., and Kjeldgaard, M. (1991). Improved methods for building protein models in electron density maps and the location of errors in these models. Acta Crystallogr. A *47*, 110–119.

Kiffe, M., Schummer, D., and Hofle, G. (1997). Chemical modification of the antifungal macrolide soraphen A1a: deoxygenation in the south-east ring segment. Liebigs Ann., 245–252.

Kondo, S., Nakajima, Y., Sugio, S., Yong-Biao, J., Sueda, S., and Kondo, H. (2004). Structure of the biotin carboxylase subunit of pyruvate carboxylase from Aquifex aeolicus at 2.2 Å resolution. Acta Crystallogr. D Biol. Crystallogr. *60*, 486–492.

Lenhard, J.M., and Gottschalk, W.K. (2002). Preclinical developments in type 2 diabetes. Adv. Drug Deliv. Rev. *54*, 1199–1212.

Ligon, J., Hill, S., Beck, J., Zirkle, R., Molnar, I., Zawodny, J., Money, S., and Schupp, T. (2002). Characterization of the biosynthetic gene cluster for the antifungal polyketide soraphen A from Sorangium cellulosum So ce26. Gene *285*, 257–267.

Loubinoux, B., Sinnes, J.-L., and O'Sullivan, A.C. (1995a). Synthesis of substructures of soraphen A: formation of the enolate of benzyl propionate. J. Chem. Soc. Perkin Trans *1*, 521–526.

Loubinoux, B., Sinnes, J.-L., O'Sullivan, A.C., and Winkler, T. (1995b). The enantioselective synthesis of simplified southern-half fragments of soraphen A. Tetrahedron *51*, 3549–3558.

Loubinoux, B., Sinnes, J.-L., O'Sullivan, A.C., and Winkler, T. (1995c). The enantioselective synthesis of the "southern part" of soraphen A. Helv. Chim. Acta *78*, 122–126.

Loubinoux, B., Sinnes, J.-L., O'Sullivan, A.C., and Winkler, T. (1995d). Synthesis of southern-part models of soraphen A. J. Org. Chem. *60*, 953–959.

McGarry, J.D., and Brown, N.F. (1997). The mitochondrial carnitine palmitoyltransferase system. From concept to molecular analysis. Eur. J. Biochem. *244*, 1–14.

Nicholls, A., Sharp, K.A., and Honig, B. (1991). Protein folding and association: insights from the interfacial and thermodynamic properties of hydrocarbons. Proteins *11*, 281–296.

Otwinowski, Z., and Minor, W. (1997). Processing of X-ray diffraction data collected in oscillation mode. Methods Enzymol. *276*, 307–326.

Pridzun, L. (1991). Untersuchungen zum Wirkungsmechanismus von Soraphen A. Ph.D. thesis. Technical University of Braunschweig, Braunschweig, Germany.

Pridzun, L., Sasse, F., and Reichenbach, H. (1995). Inhibition of fungal acetyl-CoA carboxylase: a novel target discovered with the myxobacterial compound soraphen. In Antifungal Agents, G.K. Dixon, L.G. Copping, and D.W. Hollomon, eds. (Oxford, UK: BIOS Scientific Publishers Ltd.), pp. 99–109.

Ramsay, R.R., Gandour, R.D., and van der Leij, F.R. (2001). Molecular enzymology of carnitine transfer and transport. Biochim. Biophys. Acta *1546*, 21–43.

Rendina, A.R., Felts, J.M., Beaudoin, J.D., Craig-Kennard, A.C., Look, L.L., Paraskos, S.L., and Hagenah, J.A. (1988). Kinetic characterization, stereoselectivity, and species selectivity of the inhibition of plant acetyl-CoA carboxylase by the aryloxyphenoxypropionic acid grass herbicides. Arch. Biochem. Biophys. *265*, 219–225.

Schummer, D., Jahn, T., and Hofle, G. (1995). Synthesis of soraphen analogues by substitution of the phenyl-C-17 ring segment of soraphen A1a. Liebigs Ann., 803–816.

Terwilliger, T.C., and Berendzen, J. (1999). Automated structure solution for MIR and MAD. Acta Crystallogr. D Biol. Crystallogr. *55*, 849–861.

Thoden, J.B., Blanchard, C.Z., Holden, H.M., and Waldrop, G.L. (2000). Movement of the biotin carboxylase B-domain as a result of ATP binding. J. Biol. Chem. *275*, 16183–16190.

Vahlensieck, H.F., and Hinnen, A. (1997). Soraphen A resistant fungi and acetyl-CoA carboxylase. U.S. patent 5,641,666.

Vahlensieck, H.F., Pridzun, L., Reichenbach, H., and Hinnen, A. (1994). Identification of the yeast ACC1 gene product (acetyl-CoA carboxylase) as the target of the polyketide fungicide soraphen A. Curr. Genet. *25*, 95–100.

Wakil, S.J., Stoops, J.K., and Joshi, V.C. (1983). Fatty acid synthesis and its regulation. Annu. Rev. Biochem. *52*, 537–579.

Waldrop, G.L., Rayment, I., and Holden, H.M. (1994). Three-dimensional structure of the biotin carboxylase subunit of acetyl-CoA carboxylase. Biochemistry *33*, 10249–10256.

Walsh, C.T. (2004). Polyketide and nonribosomal peptide antibiotics: modularity and versatility. Science *303*, 1805–1810.

Weatherly, S.C., Volrath, S.L., and Elich, T.D. (2004). Expression and characterization of recombinant fungal acetyl-CoA carboxylase and isolation of a soraphen-binding domain. Biochem. J. *380*, 105–110.

Zagnitko, O., Jelenska, J., Tevzadze, G., Haselkorn, R., and Gornicki, P. (2001). An isoleucine/leucine residue in the carboxyltransferase domain of acetyl-CoA carboxylase is critical for interaction with aryloxyphenoxypropionate and cyclohexanedione inhibitors. Proc. Natl. Acad. Sci. USA *98*, 6617–6622.

Zhang, H., Yang, Z., Shen, Y., and Tong, L. (2003). Crystal structure of the carboxyltransferase domain of acetyl-coenzyme A carboxylase. Science *299*, 2064–2067.

Zhang, H., Tweel, B., Li, J., and Tong, L. (2004a). Crystal structure of the carboxyltransferase domain of acetyl-coenzyme A carboxylase in complex with CP-640186. Structure *12*, 1683–1691.

Zhang, H., Tweel, B., and Tong, L. (2004b). Molecular basis for the inhibition of the carboxyltransferase domain of acetyl-coenzyme A carboxylase by haloxyfop and diclofop. Proc. Natl. Acad. Sci. USA *101*, 5910–5915.

Accession Numbers

The structures of the soraphen complex and the free enzyme have been deposited in the Protein Data Bank under ID codes 1W93 and 1W96.